The Globular Tail Domain of Myosin Va Functions as an Inhibitor of the Myosin Va Motor*

Xiang-dong Li[‡1], **Hyun Suk Jung**[§], **Katsuhide Mabuchi**[¶], **Roger Craig**[§], **and Mitsuo Ikebe**[‡]

From the Departments of [‡]Physiology and [§]Cell Biology, University of Massachusetts Medical School, Worcester, Massachusetts 01655 and the [¶]Muscle Research Group, Boston Biomedical Research Institute, Watertown, Massachusetts 02472

The actin-activated ATPase activity of full-length mammalian myosin Va is well regulated by Ca^{2+}, whereas that of truncated myosin Va without the C-terminal globular tail domain (GTD) is not. Here, we have found that exogenous GTD is capable of inhibiting the actin-activated ATPase activity of GTD-deleted myosin Va. A series of truncated constructs of myosin Va further showed that the entire length of the first coiled-coil (coil-1) of the tail domain is critical for GTD-dependent regulation of myosin Va and that deletion of 58 residues from the C-terminal end of coil-1 markedly hampered regulation. Negative staining electron microscopy revealed that GTD-deleted myosin Va formed a "Y"-shaped structure, which was converted to a triangular shape, similar to the structure of full-length myosin Va in the inhibited state, by addition of exogenous GTD. In contrast, the triangular shape was not observed when the C-terminal 58 residues of coil-1 were deleted, even in the presence of exogenous GTD. Based on these results, we propose a model for the formation of the inhibited state of myosin Va. GTD binds to the C-terminal end of coil-1. The neck-tail junction of myosin Va is flexible, and the long neck enables the head domain to reach the GTD associated with the end of coil-1. Once the head interacts with the GTD, the triangular inhibited conformation is stabilized. Consistent with this model, we found that shortening of the neck of myosin Va by two IQ motifs abolished the regulation by GTD, whereas regulation was partially restored by shortening of coil-1 by an amount comparable to that of the two IQ motifs.

Class V myosin is considered one of the oldest classes of myosin, being distributed from low eukaryotes, such as yeast, to vertebrate cells (1, 2). In mammalian cells, there are three distinct subclasses of myosin V, named myosin Va, Vb, and Vc (3–5). Myosin Va is one of the best characterized motor proteins of the myosin superfamily. Myosin Va is a processive motor, which undergoes multiple catalytic cycles coupled to multiple mechanical advances for each diffusional encounter with its actin track (6–10). This property allows single or a few myosin Va molecules to support movements of an organelle along actin filaments with a large step approximating the 36-nm pseudo repeat of the track.

Myosin Va consists of two identical heavy chains that dimerize through the formation of a coiled-coil structure to form a homodimer. At the N terminus is the motor domain containing the ATP and actin binding sites. The motor domain is followed by a neck that consists of six IQ motifs with the consensus sequence IQ*XXX*RG*XXX*R, which act as the binding sites for calmodulins or myosin light chains. The next ~500 amino acids are predicted to form a series of coiled-coils separated by several flexible regions. The last ~400 amino acids form a globular tail domain (3). This C-terminal globular tail domain (GTD),[2] in conjunction with a portion of the coiled-coil region, mediates myosin Va binding to specific membrane-bound organelles such as melanosomes (11).

One of the most important questions is how the motor function of myosin Va is regulated. If myosin Va were constantly active, then the high concentrations of myosin Va found in brain (3) would consume substantial amounts of ATP. Therefore, it is desirable that the mechanoenzymatic activities of myosin Va is regulated *in vivo*. However, the molecular mechanism of myosin Va regulation is not well understood.

The ATPase activities of tissue-isolated myosin Va (3, 12) and baculovirus-expressed full-length myosin Va (13, 14) are well regulated, the actin-activated ATPase activity of myosin Va being significantly increased by micromolar concentrations of Ca^{2+}. Sedimentation velocity analysis showed that the myosin Va undergoes a Ca^{2+}-induced conformational transition from 14 S to 11 S (12–14). Electron microscopy revealed that at low ionic strength, myosin Va has an extended conformation in high Ca^{2+} whereas it forms a folded shape in the presence of EGTA, in which the tail domain is folded back toward the head (12). The conformational transition is closely correlated with activation of the actin-activated ATPase activity of myosin Va (13). On the other hand, truncated myosin Va without the globular tail domain is not regulated by Ca^{2+} (15, 16) and does not undergo a large conformational transition like full-length myosin Va (13, 14). These results suggest that the tail domain plays a key role in the Ca^{2+}-dependent regulation of myosin Va, by inhibiting the ATPase of the head (12–14). In this model, myosin Va in the inhibited state is in a folded conformation such

---

[1] To whom correspondence should be addressed: Dept. of Physiology, University of Massachusetts Medical School, 55 Lake Ave. N., Worcester, MA 01655. Tel.: 1-508-856-2338; Fax: 1-508-856-5997; E-mail: Xiangdong.Li@umassmed.edu.

[2] The abbreviations used are: GTD, C-terminal globular tail domain of myosin Va; DTT, dithiothreitol; McM5, melanocyte-type myosin Va; PEP, phosphoenol pyruvate; TCEP, Tris [2-carboxyethyl]phosphine; Ni-NTA, nickel-nitrilotriacetic acid; aa, amino acids; MOPS, 4-morpholinepropanesulfonic acid.
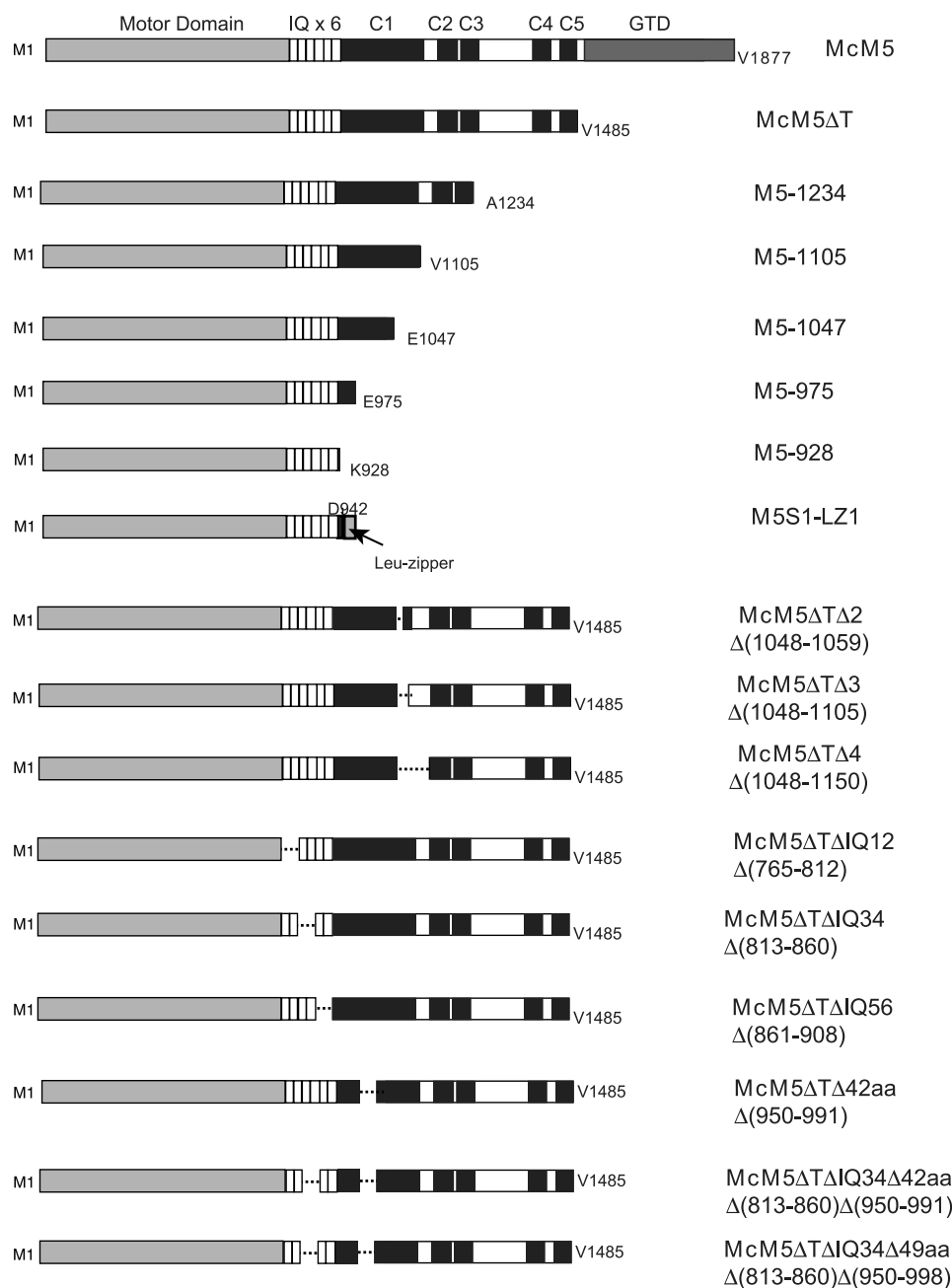
FIGURE 1. **Domains of mouse melanocyte-type myosin Va (McM5) and the truncated constructs studied in this article.** *Top*, the different functional domains of McM5, including the motor domain, neck (IQ motifs), and tail. The six light chain binding IQ motifs in the neck are shown as *stippled boxes*, five coiled-coil regions (*C1–C5*) as *black rectangles*, and the C-terminal GTD as *gray rectangles*. *Bottom*, truncated myosin Va constructs studied in this article. *Broken line* represents the internal deletion. The amino acid numbers of the constructs are indicated.

interaction between the tail and head domains of myosin Va, thus relieving the inhibitory effect of the tail domain (17).

In this study, we further investigated the molecular mechanism of the regulation of the motor activity of myosin Va. Our results indicate that the C-terminal globular tail domain of myosin Va directly binds to the head domain, thus inhibiting motor function. Furthermore, our results suggest that the lengths of the neck domain and the first long coiled-coil domain structurally coordinate the binding between the head and the tail domains, and thus are critical for the regulation of myosin Va motor activity.

EXPERIMENTAL PROCEDURES

Materials—Restriction enzymes and modifying enzymes were purchased from New England Biolabs (Beverly, MA), unless indicated otherwise. Pfu Ultra High-Fidelity DNA polymerase was purchased from Stratagene (La Jolla, CA). Oligonucleotides were synthesized by Invitrogen (Carlsbad, CA). Actin was prepared from rabbit skeletal muscle acetone powder according to Spudich and Watt (22). Recombinant calmodulin of *Xenopus* oocyte (23) was expressed and purified according to a published method (24). Nickel-nitrilotriacetic acid (Ni-NTA)-agarose and mouse monoclonal antibody recognizing penta-His (anti-His tag) were purchased from Qiagen (Hilden, Germany). Anti-FLAG M2 antibody, anti-FLAG M2 affinity gel, FLAG peptide (Asp-Tyr-Lys-Asp-Asp-Asp-Lys), phosphoenol pyruvate, 2,4-dinitrophenyl-hydrazine, and pyruvate kinase were from Sigma. Phenyl-Sepharose and Sephacryl S-300 were purchased from Amersham Biosciences. Anti-M5T antibody, an antibody recognizing the C-terminal 22 amino acid residues of myosin Va, was provided by Dr. Jack L. Leonard, Department of Physiology, University of Massachusetts Medical School (25).

Myosin Va Expression Vectors—Murine melanocyte-type myosin Va (McM5), was subcloned into baculovirus transfer vector pFastBac (Invitrogen) as described before (13, 17). To facilitate the purification, an N-terminal tag (MSYYH HHHHH DYKDD DDKNI PTTEN LYFQG AMGIR NSKAY VDELT

that the tail domain interacts with and inhibits the myosin Va motor activity. Cargo binding, high Ca^{2+}, and/or phosphorylation may reduce the interaction between the head and tail domains, thus activating its activity.

Consistent with this model, we recently found that the actin-activated ATPase activity of melanocyte-type myosin Va is significantly activated by the binding of melanophilin (17), an organelle receptor for myosin Va in mouse melanocytes (18–21). Because myosin Va binds to melanophilin through its tail domain, we proposed that this interaction interferes with the
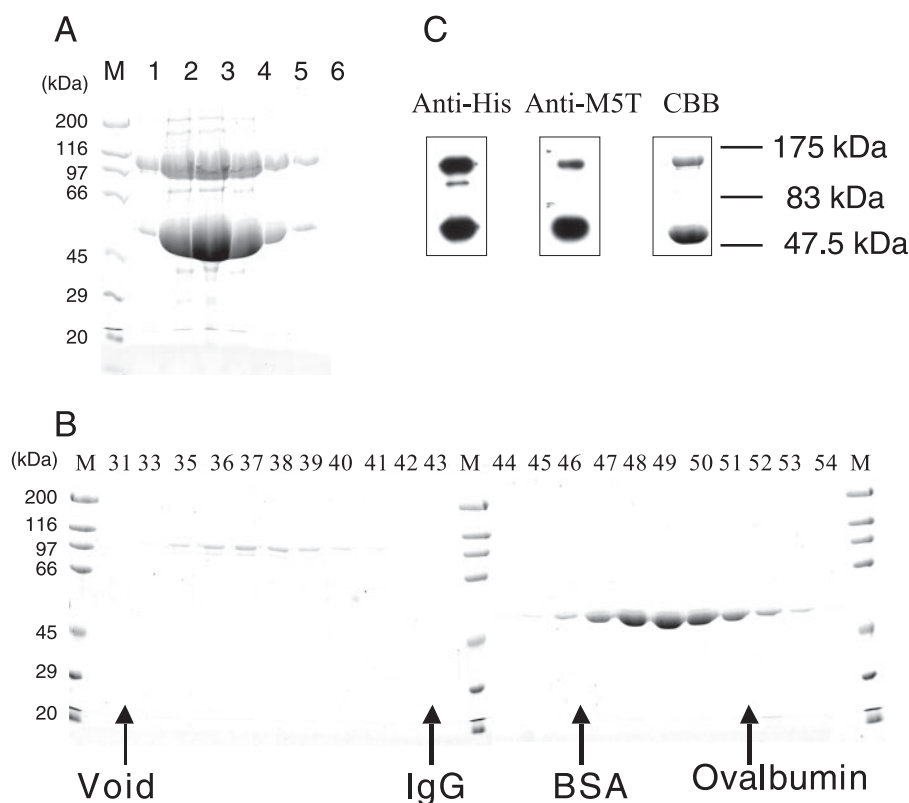
FIGURE 2. **Preparation of C-terminal globular tail domain of myosin Va (GTD).** N-terminal His-tagged GTD was expressed in baculovirus expression system, and purified by Ni-NTA-agarose chromatography and size-exclusive chromatography (Sephacryl S-300, 1.5 × 60 cm). *A*, SDS-PAGE of eluted fractions from Ni-NTA-agarose chromatography. *Lane M* shows the molecular mass markers; *lanes 1–6* correspond to the fractions eluted from Ni-NTA-agarose column. *B*, SDS-PAGE of the fractions from Sephacryl S-300. The number on each lane (31–54) represents the fraction eluted from Sephacryl S-300. *Arrows* indicate the elution peaks of void, IgG (150 kDa), bovine serum albumin (*BSA*, 66 kDa), and ovalbumin (43 kDa), respectively. *C*, elution from Ni-NTA-agarose chromatography was subjected to SDS-PAGE and Western blots (anti-His tag or anti-M5T) or Coomassie Brilliant Blue (*CBB*) staining analysis.

HCl, pH 7.5), the cell pellets were lysed with sonication in 50 ml of lysis buffer (50 mM Tris-HCl, pH 7.5, 15 mM imidazole-HCl, pH7.5, 0.3 M NaCl, 5 mM MgCl$_2$, 1 mM EGTA, 0.02% NaN$_3$, 5 mM ATP, 5 mM 2-mercaptoethanol, 10 μg/ml leupeptin, 0.2 mg/ml trypsin inhibitor (Egg), and 0.5% Triton X-100). After centrifugation at 120,000 × g for 30 min, the supernatant was incubated with 4.0 ml of Ni-NTA-agarose affinity resin in a 50-ml conical tube on a rotating wheel in a cold room for 2 h. The resin suspension was then loaded on a column (1 × 10 cm) and washed with 30 ml of solution A (50 mM Tris-HCl, pH 7.5, 15 mM imidazole-HCl pH7.5, 0.3 M NaCl, 0.2 mM EGTA, 2 μg/ml leupeptin, and 5 mM 2-mercaptoethanol). The protein bound to the resin was eluted with 0.25 M imidazole in solution A. SDS-PAGE showed that the eluate from the Ni-NTA-agarose column contained two bands with apparent molecular masses of 100 kDa and 50 kDa (Fig. 2*A*). The calculated molecular mass of GTD is 50 kDa. It therefore appeared that the lower and upper bands in SDS-PAGE might be monomeric and dimeric GTD, respectively. Western blot showed that both bands were recognized by anti-His antibody and anti-M5T antibody (Fig. 2*C*). To separate the two bands, the eluate from Ni-NTA-agarose chromatography was subjected to size-exclusion chromatography. About 4 ml of the eluate from Ni-NTA-agarose was loaded onto a Sephacryl S-300 column (1.5 × 60 cm) pre-equilibrated with Solution D (0.2 M NaCl, 5 mM Tris-HCl, pH 7.5, 1 mM DTT). The fractions 30–54 (1.5 ml per fraction) were collected and subjected to SDS-PAGE (Fig. 2*B*). The fractions containing high concentrations of monomeric GTD were pooled. The concentration of GTD was determined by the absorbance at 280 nm (1 A_{280} equal to 1.35 mg/ml GTD). About 10 mg of monomeric GTD could be obtained in one preparation.

The nature of the putative "dimeric GTD" is not clear. Because there are 8 cysteine residues in GTD, we suspected that some GTD might have dimerized by cross-linking through intermolecular disulfide bonds. However, the migration of the "dimeric GTD" in SDS-PAGE did not change even when it was treated with high concentrations of reducing reagents (0.1 M 2-mercaptoethanol, 0.1 M DTT, or 25 mM TCEP, data not shown). In size-exclusion chromatography (Fig. 2*B*), the dimeric GTD eluted far ahead of IgG (molecular mass of 150 kDa), suggesting that it may be an oligomer of dimeric GTD.

SPA), containing a sequence of His$_6$ tag and FLAG tag, was added to McM5. C-terminal-truncated myosin Va were produced by introducing a stop codon at various nucleotide sites of McM5 (Fig. 1). M5S1-LZ1 was produced by replacing the last 33 residues (Tyr[943]–Glu[975]) of M5-975 with the 32 residues of GCN4 leucine zipper (MKQLEDK VEELLSK NYHLENE VARLKKL VGER) by using overlapping PCR. GTD-deleted myosin Va with internal deletions, including McM5ΔTΔ2, McM5ΔTΔ3, McM5ΔTΔ4, McM5ΔTΔIQ12, McM5ΔTΔIQ34 McM5ΔTΔIQ56, McM5ΔTΔIQ34Δ49aa, McM5ΔTΔ42aa, and McM5ΔTΔIQ34Δ42aa, were produced by overlapping PCR as described previously (17). The cDNA coding the GTD (Gly[1468]–Val[1877]) was constructed by conventional PCR and subcloned in-frame to pFastBacHTb (Invitrogen). An N-terminal tag (MSYYH HHHHH DNIPT TENLY FQGAM GS) containing His$_6$ tag was added to GTD. Recombinant baculoviruses were prepared as described previously (13).

Expression and Purification of Myosin Va Constructs—GTD was expressed in Sf9 cells and purified by Ni-NTA-agarose affinity chromatography and size-exclusion chromatography. To express GTD, 400 ml of Sf9 cells (suspension culture) was infected with baculovirus expressing GTD, and cultured in 1 liter of medium at 27 °C for 3 days. After harvesting and washing with 4 mM EGTA in TBS (0.15 M NaCl, and 50 mM Tris-
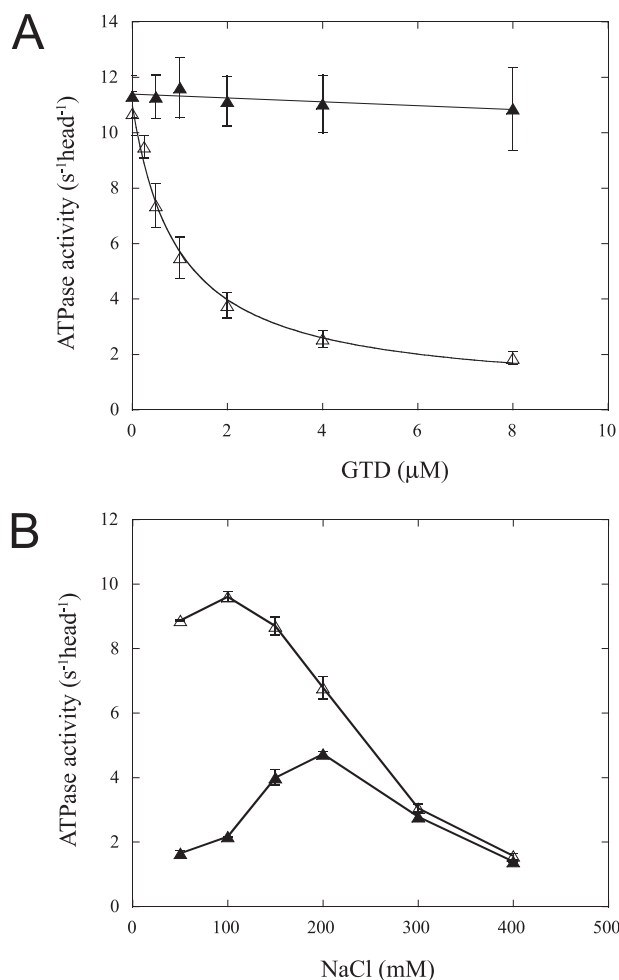
FIGURE 3. **Effect of exogenous GTD on the actin-activated ATPase activity of GTD-deleted myosin Va (McM5ΔT).** *A*, effects of GTD on the actin-activated ATPase activity of McM5ΔT under EGTA (*open triangles*) and pCa5 (*closed triangles*) conditions. The experiments were conducted in a solution containing 20 mM MOPS-KOH, pH 7.0, 0.1 M NaCl, 1 mM MgCl₂, 1 mM DTT, 0.25 mg/ml bovine serum albumin, 12 μM calmodulin, 0.5 mM ATP, 2.5 mM PEP, 20 units/ml pyruvate kinase, 40 μM actin, 25–50 nM McM5ΔT, various concentrations of GTD, and 1 mM EGTA at 25 °C (EGTA condition). 1 mM EGTA was replaced with 1.03 mM EGTA and 1 mM CaCl₂ for the pCa5 condition. The actin-activated ATPase activities of McM5ΔT are plotted as a function of GTD concentration. The fit to a hyperbola defines an affinity of GTD for McM5ΔT in EGTA as 0.88 ± 0.11 μM (five independent assays). *B*, affect of ionic strength on the actin-activated ATPase activity of McM5ΔT under the EGTA condition. *Open triangles*, in the absence of GTD; *closed triangles*, in the presence of 4 μM GTD. Data are the average of two independent assays.

Whatever the nature of the 100-kDa band, all following experiments were done with the monomeric GTD.

Full-length myosin Va and the truncated mutants were expressed in Sf9 cells by co-infection with recombinant baculovirus expressing myosin Va and calmodulin. Expressed myosin Va was purified by anti-FLAG M2 affinity gel as described previously (13), except that the purified myosin Va samples were dialyzed against 5 mM Tris-HCl (pH 7.5 at 20 °C), 0.2 M NaCl, 1 mM EGTA, 1 mM DTT, and 10% sucrose on ice overnight. The purified myosin Va samples, in an aliquot of 100 μl in PCR tube, were quick-frozen in liquid nitrogen and stored at −80 °C. The concentration of myosin Va was determined by Coomassie Brilliant Blue R250 staining of SDS-PAGE gels (7.5–20%) using smooth muscle myosin heavy chain as a standard as
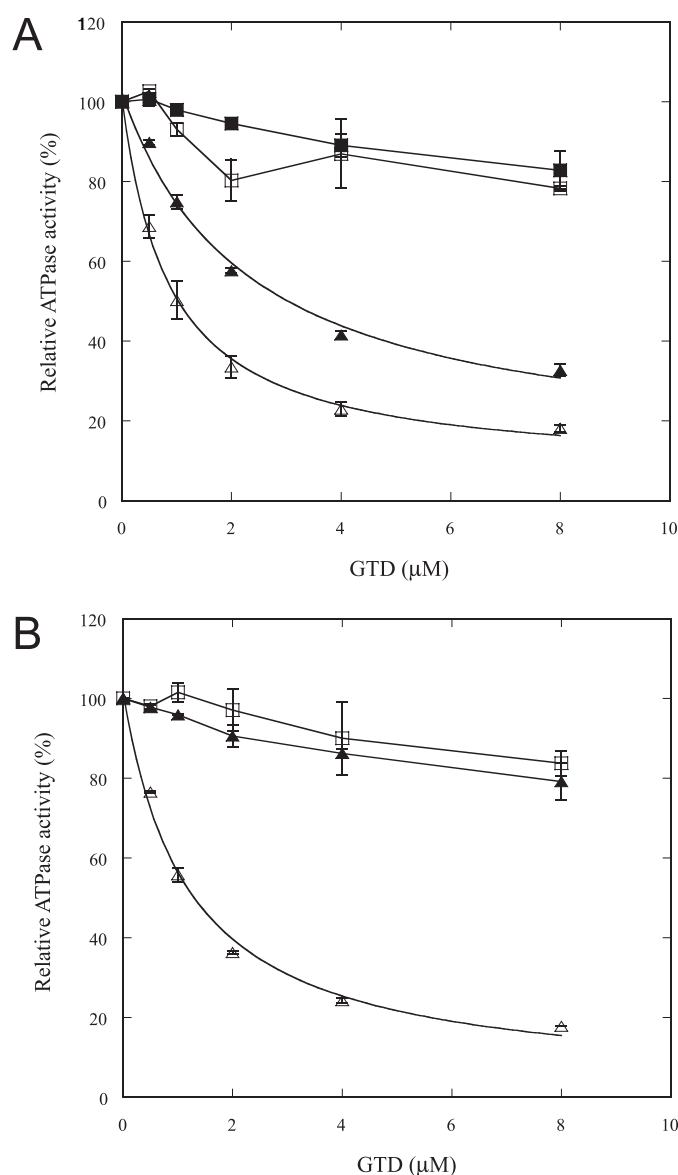
FIGURE 4. **Effect of C-terminal truncation of myosin Va on the inhibitory effect of GTD.** *A*, actin-activated ATPase activities of McM5ΔT (*open triangles*), M5-1105 (*closed triangles*), M5-1047 (*open squares*), and M5-928 (*closed squares*) under the EGTA condition in the presence of various concentrations of GTD. *B*, actin-activated ATPase activities of M5-1234 (*open triangles*), M5-975 (*closed triangles*), and M5S1-LZ1 (*open squares*) under the EGTA condition in the presence of various concentrations of GTD. The *y*-axis represents the relative activities of each construct in the presence of GDT to that in the absence of GTD, which are 10.66 ± 0.89, 10.68 ± 0.96, 10.06 ± 0.84, 10.63 ± 0.40, 8.65 ± 0.44, 8.37 ± 0.10, and 10.21 ± 0.23 s⁻¹ head⁻¹ for McM5ΔT, M5-1234, M5-1105, M5-1047, M5-975, M5-928, and M5S1-LZ1, respectively. (All data are the average of two independent assays except that of McM5ΔT, which are the averages of five independent assays.) The actin-activated ATPase activities of McM5ΔT, M5-1234, and M5-1105 in the presence of various concentrations of GTD were fit to a hyperbola, defining an affinity of GTD for McM5ΔT as 0.88 ± 0.11 μM (n = 5); for M5-1234 as 1.20 ± 0.05 μM (n = 2); and for M5-1105 as 2.33 ± 0.04 μM (n = 2).

described previously (13). To calculate the molar concentration of the expressed protein, the following molecular masses (in kDa) were used: 224 (McM5), 177 (McM5ΔT), 149 (M5-1234), 135 (M5-1105), 128 (M5-1047), 114 (M5-975), 114 (M5-928), 119 (M5S1-LZ1), 176 (McM5ΔTΔ2), 170 (McM5ΔTΔ3), 165 (McM5ΔTΔ4), 171 (McM5ΔTΔIQ12), 171 (McM5ΔTΔIQ34) 171 (McM5ΔTΔIQ56), 172 (McM5ΔT
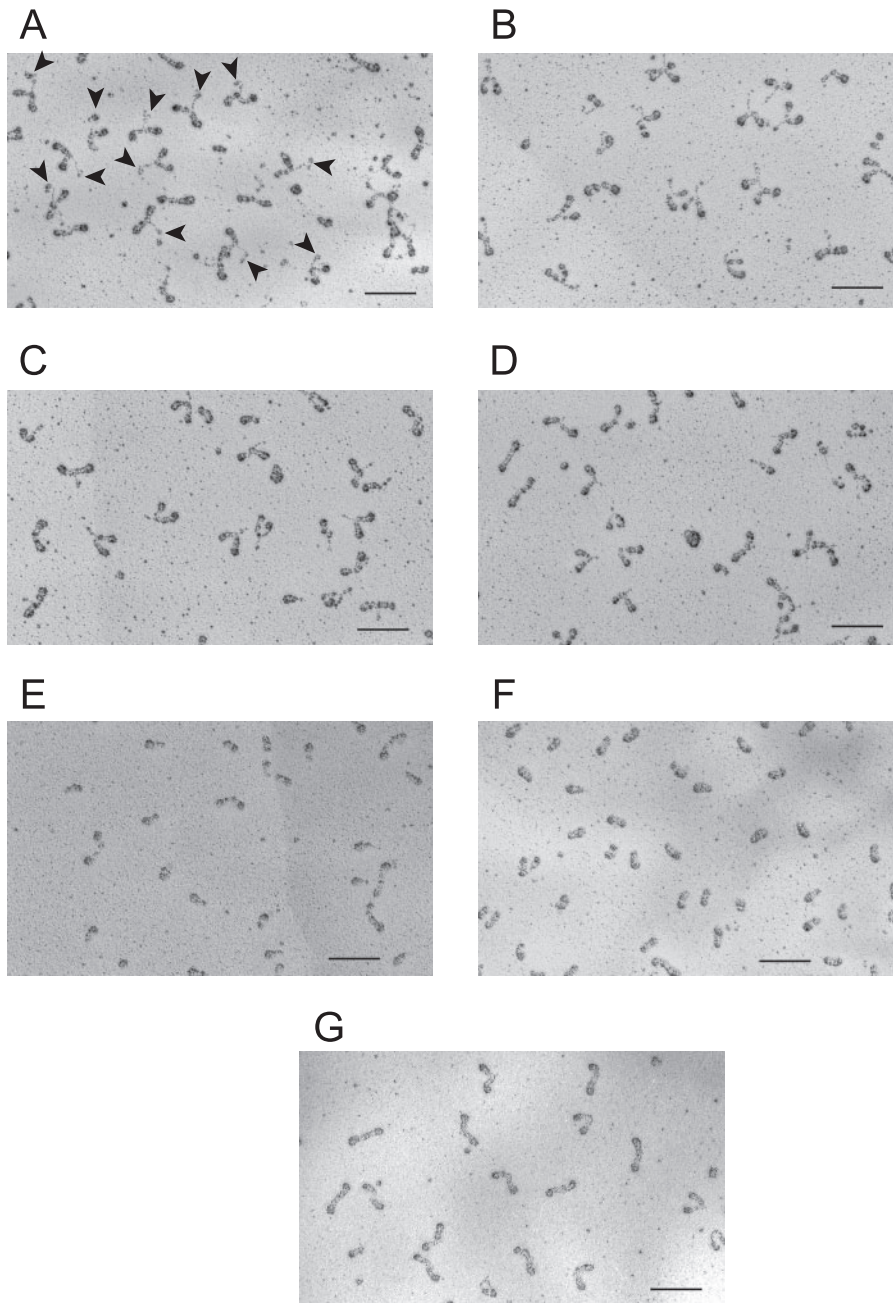
FIGURE 5. **Rotary-shadowing electron microscopy of various truncated myosin Va.** All truncated myosin Va constructs were diluted to about 4 nM by EGTA-600 before absorbing onto mica. *A*, McM5ΔT; *B*, M5-1234; *C*, M5-1105; *D*, M5-1047; *E*, M5-975; *F*, M5-928; and *G*, M5S1-LZ1. The *arrowheads* in *A* indicate the small globular domain at the end of the tail of McM5ΔT. The length of the stalk of McM5ΔT is 30.5 ± 4.8 nm (*n* = 72), and that of the tail of M5-1105 is 31.3 ± 2.5 nm (*n* = 51). *Scale bar*: 100 nm.

or truncated myosin Va was diluted to 20 nM with 0.15 M sodium acetate, 1 mM EGTA, 2 mM MgCl$_2$, 10 mM MOPS (pH 7.0) at room temperature. Five microliters of the solution were applied to UV-treated or glow-discharged, carbon-coated grids, and immediately stained with 1% uranyl acetate (27). The same procedure was used for the specimens made by mixing 20 nM truncated myosin Va with 2 μM GTD for 10 min. Negatively stained grids were examined in a CM120 electron microscope (FEI, Hillsboro, OR), fitted with an anti-contamination device cooled by liquid nitrogen, and operated at 120 kV. Micrographs were recorded on an F224HD slow scan CCD camera (TVIPS, Gauting, Germany) at a magnification of 65,000 (0.37 nm/pixel).

Other Assays—The ATPase activity of myosin Va was measured using an ATP regeneration system at 25 °C as described before (13). Reaction solution, except ATP, was mixed and preincubated at 25 °C for 10 min before adding ATP to start the reaction. SDS-PAGE and Western blot were as described previously (13).

RESULTS

Exogenous GTD Inhibits the ATPase Activity of GTD-deleted Myosin Va (McM5ΔT)—As described in the introduction, the actin-activated ATPase activity of truncated myosin Va without the C-terminal GTD is not regulated by Ca^{2+}, whereas that of full-length myosin Va is (15, 16). Regulation is abolished by deleting just the GTD (the construct of McM5ΔT, see Fig. 1) (14). These results suggest that the GTD is necessary to inhibit the actin-activated ATPase activity of myosin Va.

To determine whether exogenous GTD inhibits the function of the myosin Va motor domain, we measured the actin-activated ATPase activity of McM5ΔT (Fig. 1) in the presence of exogenous GTD. The inhibition of ATPase activity was dose-dependent, and the apparent affinity between McM5ΔT and GTD was 0.88 μM (Fig. 3*A*). The actin-activated ATPase activity of McM5ΔT in the presence of 8 μM GTD was similar to that of full-length myosin Va under EGTA conditions, which was 1.75 head^{-1} s^{-1} under similar conditions (13), suggesting that McM5ΔT was changed to an inhibited state in the presence of

Δ49aa), 172 (McM5ΔTΔ42aa), 166 (McM5ΔTΔIQ34Δ49aa), 166 (McM5ΔTΔIQ34Δ42aa), and 50 (GTD).

Electron Microscopy—Rotary metal-shadowing electron microscopy of myosin Va was performed as described previously (13). Briefly, myosin Va samples, diluted to about 4 nM in EGTA-600 solution (1 mM MgCl$_2$, 30% glycerol, 1 mM EGTA, 600 mM ammonium acetate, pH 7.0), were absorbed onto a freshly cleaved mica surface for 30 s. Unbound proteins were rinsed away, and then the specimen was stabilized by brief exposure to uranyl acetate (26) before shadowing. For negative staining, full-length
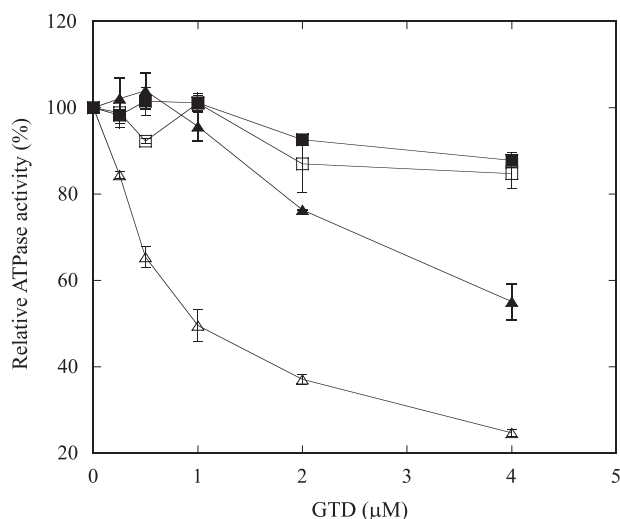
FIGURE 6. **Deletion of the coil-1/hinge region of McM5ΔT on the inhibitory effect of GTD.** McM5ΔTΔ2, McM5ΔTΔ3, and McM5ΔTΔ4 were produced by deletions of the coil-1/hinge region of McM5ΔT as depicted in Fig. 1. The actin-activated ATPase activities of truncated myosin Va constructs were measured as described in Fig. 4. The *y*-axis represents the relative activities of each construct in the presence of GDT to that in the absence of GTD, which are 10.97 ± 0.02, 10.14 ± 0.29, 9.85 ± 0.07, and 7.54 ± 0.28 s^{-1} head^{-1} for McM5ΔT, McM5ΔTΔ2, McM5ΔTΔ3, and McM5ΔTΔ4, respectively (average of two independent assays). *Open triangles*, McM5ΔT; *closed triangles*, McM5ΔTΔ2; *open squares*, McM5ΔTΔ3; and *closed squares*, McM5ΔTΔ4.

exogenous GTD. Similar to full-length myosin Va, the activity of McM5ΔT was not inhibited by GTD under high Ca^{2+} conditions (Fig. 3*A*).

The inhibitory effect of GTD on McM5ΔT was very sensitive to ionic strength. As shown in Fig. 3*B*, with an increase of NaCl from 100 mM to 400 mM, the ATPase activity of McM5ΔT in the absence of GTD sharply decreased, whereas that of McM5ΔT in the presence of GTD was bell-shaped with an increase in ionic strength. Overall, the inhibitory effect of GTD on McM5ΔT decreases with an increase in ionic strength. When the NaCl concentration is over 300 mM, GTD has virtually no inhibitory effect. These results suggest that GTD-dependent inhibition of the ATPase activity of McM5ΔT depends on ionic interaction.

The First Long Coiled-coil Segment Is Essential for Inhibition of the ATPase Activity of Myosin Va Motor Domain—The motor domain and neck of myosin Va are connected to the GTD by a series of coiled-coil domains interrupted by a number of flexible regions (Fig. 1). The number and length of predicted coiled-coils varies among different isoforms of myosin Va. For McM5, five coiled-coils separated by four flexible regions are predicted by Paircoil (28). To investigate which portion of the tail domain is essential for regulation by GTD, we made a series of C-terminal truncation mutants of myosin Va (Fig. 1), and examined the inhibitory effect of GTD on the actin-activated ATPase activity of the constructs. As shown in Fig. 4, the ATPase activity of M5-1234 was potently inhibited by GTD with an apparent affinity of 1.2 μM, which is similar to that of McM5ΔT. The inhibition of the actin-activated ATPase activity of M5-1105 by GTD was slightly less than that of M5-1234. By contrast, the actin-activated ATPase activities of M5-928, M5-975, and M5-1047 were not effectively inhibited by GTD. These results indicate that the first long coiled-coil (coil-1) is

critical for regulation, whereas the distal tail portion, *i.e.* coil-2 to coil-5, is not essential for inhibition by GTD. These results could be explained in three ways. The first is that the specific sequence of the C-terminal portion of coil-1 is essential for regulation by GTD. Second, the double-headed structure is critical for regulation and deletion of the C-terminal portion of coil-1 destabilizes the double-headed structure. Third, the length of coil-1 is critical for GTD-induced inhibition of myosin Va. To examine whether the regulation of truncated myosin Va is related to the double-headed state, we visualized the molecules by rotary metal-shadowing electron microscopy. We found that the majority of the molecules of McM5ΔT, M5-1234, M5-1105, and M5-1047 were double-headed, whereas about 75% of M5-975 and most of M5-928 were single-headed (Fig. 5). These results suggest that single-headed myosin Va S1 is not regulated. On the other hand, although both M5-1105 and M5-1047 are mostly double-headed, GTD markedly inhibited the actin-activated ATPase activity of M5-1105, but only marginally inhibited that of M5-1047, suggesting that the double-headed structure is not sufficient for the regulation by GTD.

To further clarify the role of the double-headed structure, we constructed M5S1-LZ1, an artificially dimerized myosin Va S1, by replacing the C-terminal 33 amino acid residues of M5-975 with 32 amino acid residues of leucine zipper, producing a continuous, in-register coiled-coil (Fig. 1). As shown in Fig. 5*G*, the majority of M5S1-LZ1 molecules are double-headed. However, the actin-activated ATPase activity of M5S1-LZ1 is not effectively inhibited by GTD, being similar to that of M5-975 (Fig. 4), indicating that the double-headed structure is not sufficient for the regulation of myosin Va by GTD.

To investigate the role of the coil-1/hinge region on the regulation of myosin Va, we produced three McM5ΔT constructs with various deletions in this region (Fig. 1). Deletion of 1048–1059 (McM5ΔTΔ2) moderately decreased the inhibitory effect of GTD on the ATPase activity, whereas deletion of 1048–1105 (McM5ΔTΔ3) or 1048–1150 (McM5ΔTΔ4) essentially eliminated the inhibitory effect of GTD (Fig. 6). The results support the idea that the C-terminal portion of coil-1 is important for GTD-induced inhibition of ATPase activity.

In the Presence of GTD, Truncated Myosin Va Forms a Triangular Shape, Which Is Similar to Full-length Myosin Va—It was reported that full-length myosin Va forms a triangular shape at low Ca^{2+} and low ionic strength (12). This suggested that GTD directly contacts the motor domain, thus inhibiting its motor function. Because exogenous GTD inhibited the ATPase activity of McM5ΔT, we examined whether exogenous GTD and McM5ΔT formed this triangular shape. As shown in Fig. 7*B*, McM5ΔT had a T- or Y-shape in the absence of GTD (at 150 mM sodium acetate), but formed a triangular shape in its presence (Fig. 7*D*), similar to that of full-length myosin Va, McM5 (Fig. 7*A*).

Similar to McM5ΔT, M5-1105 also formed a triangular shape in the presence of GTD (Fig. 7*E*), but a T- or Y-shape in its absence (Fig. 7*C*). In contrast, we did not observe a triangular shape for either McM5ΔTΔ3 or M5-1047 even in the presence of GTD under the same conditions (data not shown). These results, in conjunction with the results that the ATPase activi-
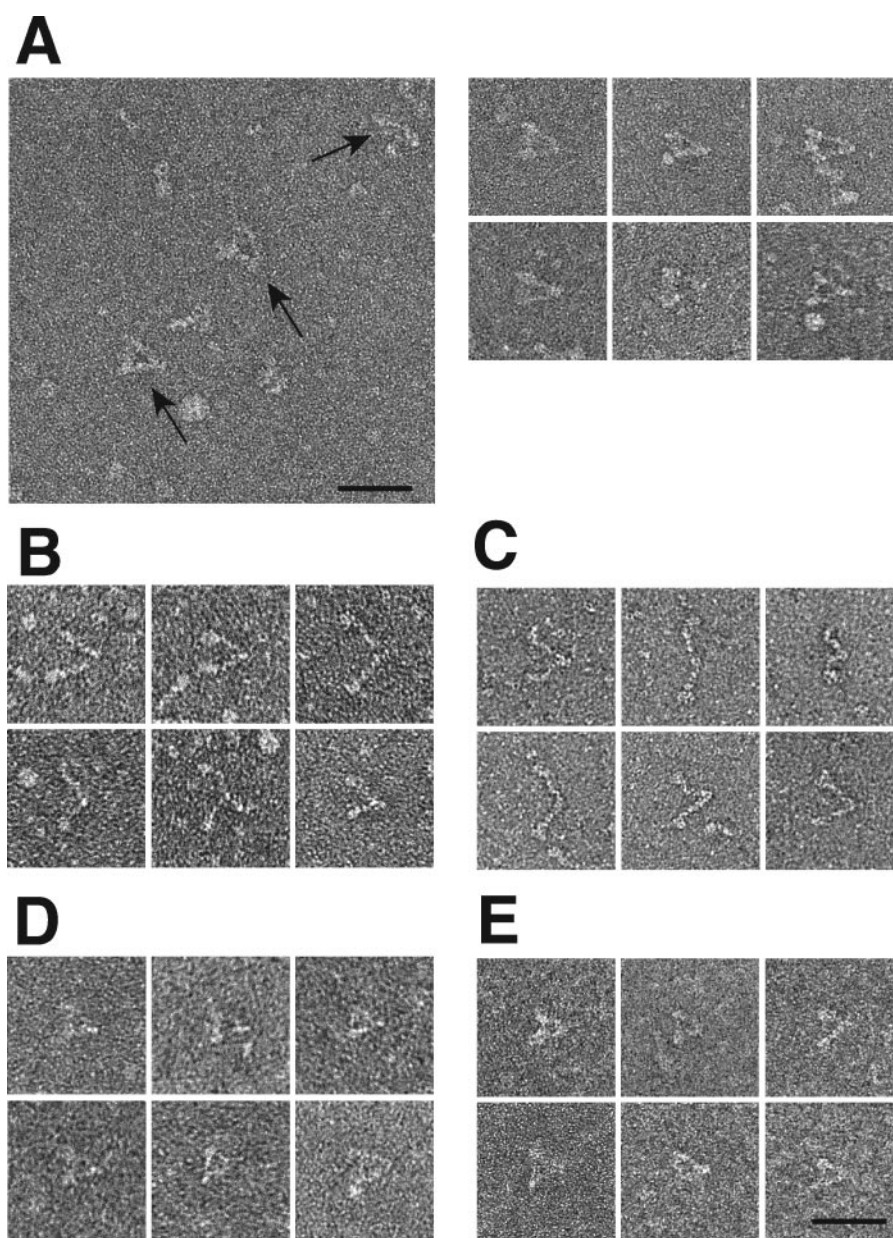
FIGURE 7. **Negatively stained images of full-length and truncated myosin Va at physiological ionic strength in EGTA and in the absence of MgATP.** *A*, field of full-length myosin Va (McM5); *arrows* indicate triangular-shaped molecules, also shown in gallery at right. *B* and *C*, gallery of truncated myosin Va, molecules, McM5ΔT and M5-1105, respectively, showing T- or Y-shaped molecules. *D* and *E*, gallery of McM5ΔT and M5-1105, respectively, in the presence of GTD, showing a *triangular shape*. Note: the molecules in *D* and *E* are less well defined because of deep staining, possibly resulting from the 100-fold molar excess of GTD used to ensure binding at the low protein concentrations required. Nevertheless, the only molecules identified in these GTD-containing specimens were triangular-shaped, similar to full-length myosin. *Scale bars*: 50 nm.

ate this hypothesis, we produced a number of constructs with various deletions of the neck region or coil-1 region (Fig. 1), and investigated their regulation by GTD. As shown in Fig. 8, McM5ΔTΔIQ34, a myosin Va mutant with its neck shortened by deleting the 3rd and 4th IQ motifs was not effectively inhibited by GTD. This result could mean that the 3rd and 4th IQ motifs, specifically, are essential for regulation, or that the intact neck is important for regulation. To evaluate these possibilities, we produced McM5ΔTΔIQ12, and McM5ΔTΔIQ56, by deleting IQ1 and IQ2 or IQ5 and IQ6 of myosin Va, respectively (Fig. 1). Similar to McM5ΔTΔIQ34, the actin-activated ATPase activity of neither McM5ΔTΔIQ12 nor McM5ΔTΔIQ56 was effectively inhibited by GTD (data not shown), indicating that the deletion of any two IQ motifs of neck disrupts the interaction between the motor domain and GTD.

The deletion of two IQ motifs shortens the neck by 7.2 nm (48 amino acid residues $\times$ 0.15 nm for each residue in the α-helix). One possible scenario is that the shortening of the neck makes it difficult for GTD, which is located 30-nm away from the joint of the two heads, to interact with the motor domain. If so, deletion of an appropriate length of the proximal region of coil-1 may restore the interaction between the motor domain and GTD.

As shown in Fig. 7, full-length myosin Va forms a triangular shape with an angle of about 40 degrees between the two heads. Therefore, shortening of the proximal coiled-coil region by about 6.77 nm (7.2 nm $\cdot$ cos (40°/2)) would restore the

triangular shape thus restoring the interaction between motor domain and GTD. The length of 6.77 nm is equivalent to 45 amino acid residues in an α-helix coiled-coil. Because the helical period of the coiled-coil is 7 amino acid residues, deletion of 49 or 42 residues would produce a continuous, in-register coiled-coil. Therefore, we deleted 950–998 (49 residues) and 950–991 (42 residues) of McM5ΔTΔIQ34 at the coil-1 region, producing McM5ΔTΔIQ34Δ49aa and McM5ΔTΔIQ34Δ42aa, respectively (Fig. 1). We found that deletion of 42 aa partially restored the regulation of McM5ΔTΔIQ34 by GTD (Fig. 8), whereas deletion of 49 aa did not (data not shown). In contrast,

ties of both McM5ΔT and M5-1105 are inhibited by GTD, whereas those of McM5ΔTΔ3 and M5-1047 are not, suggest that the triangular shape of myosin Va represents an inhibited state and confirm that GTD directly interacts with the head to inhibit the motor function of myosin Va.

The Relative Geometric Position of the Tail and the Head Is Critical for the Regulation of Myosin Va—Because the above results suggest that the triangular form represents the inhibitory state, we hypothesized that the length of the neck domain and the first long coiled-coil, as well as the proper orientation of the tail and the head are critical for inhibition by the tail binding to the head. To evalu-
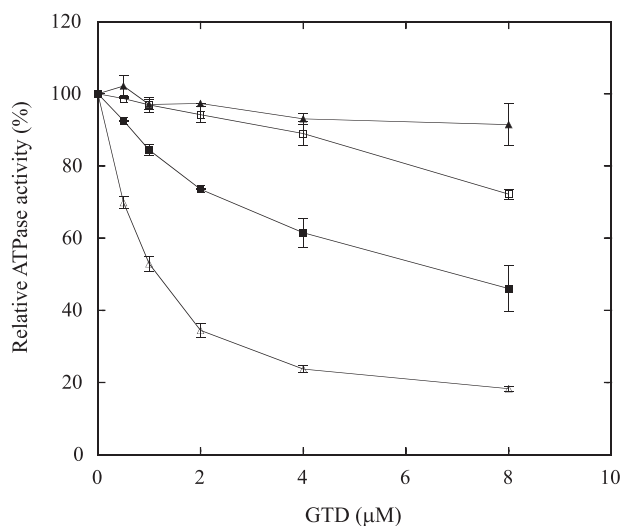
FIGURE 8. **Effect of deletion of neck and/or coil-1 of McM5ΔT on the inhibitory effect of GTD.** The actin-activated ATPase activities of truncated myosin Va were measured as described in Fig. 4. The *y*-axis represent the relative activities the relative activities of each construct in the presence of GDT to that in the absence of GTD, which are 10.99 ± 0.78, 8.46 ± 0.51, 10.81 ± 0.48, and 7.51 ± 0.28 s^{-1} head^{-1} for McM5ΔT, McM5ΔTΔIQ34, McM5ΔTΔ42aa, and McM5ΔTΔIQ34Δ42aa, respectively (average of two independent assays). *Open triangles*, McM5ΔT; *closed triangles*, McM5ΔTΔIQ34; *open squares*, McM5ΔTΔ42aa; and *closed squares*, McM5ΔTΔIQ34Δ42aa.

the deletion of 42 aa of McM5ΔT (McM5ΔTΔ42aa) markedly decreased the regulation of McM5ΔT by GTD (Fig. 8). These results support the idea that the appropriate length of neck and coil-1 of myosin Va are critical for the interaction between motor domain and GTD, and thus the regulation of myosin Va.

DISCUSSION

The Structure of the Tail Domain of Myosin Va—We examined the structure of various truncated constructs of myosin Va by electron microscopy. One of the most intriguing findings is that the tail length is much shorter than that predicted based upon a series of coiled-coil domains in the tail. The proximal portion (residues 909–1467) of the tail of myosin Va are predicted to be five coiled-coils separated by four flexible regions by Paircoil (28). The length of coil-1 (residues of 909–1105) is predicted to be 29.4 nm, and those of the other four coiled-coil helices (coil-2 to coil-5) are 6.5, 6.3, 6.8, and 5.4 nm, respectively. If these coiled-coil domains are linearly arranged to form a long stalk, the length between the joint of the two-heads to GTD would be ∼55 nm, much longer than the observed 30-nm length of the stalk of myosin Va (Fig. 5 and Ref. 3). We found a small globular structure at the end of McM5ΔT (Fig. 5*A*), which is not found for the tail of M5-1105 or M5-1234. The length of the stalk of McM5ΔT is essentially equal to that of M5-1105 tail (30.5 nm *versus* 31.3 nm) (Fig. 5). These results suggest that the four short putative coil domains do not serve as a stalk but constitute the small globular domain. This view is consistent with the earlier images of chicken myosin Va visualized by quick-freeze deep-etch electron microscopy. Cheney *et al.* (3) observed a small globule besides the globular tail domain in electron micrographs of chick brain myosin Va, and sug-

gested that this structure probably corresponds to residues of 1107–1420 of chick brain myosin Va (corresponding to 1106–1467 of McM5) (3). It has been observed that the length of tail of myosin Va is variable. Earlier images of myosin Va observed by quick-freeze deep-etch electron microscopy showed the length from the head-rod junction to the end of GTD to vary from ∼30 nm to a maximum of 75 nm (3). Rotary metal-shadowed images of mouse myosin Va show that the distance between the head-rod junction and GTD is shorter in low ionic strength than in high ionic strength (14). Those observations suggest that the small globular domain formed by coil-2 to coil-5 might be extended under certain conditions.

The Structure of the Inhibited State of Myosin Va—In the present study, we found that exogenous GTD inhibits the actin-activated ATPase activity of unregulated HMM-like myosin Va constructs. The results clearly indicate that GTD functions as an inhibitor domain of myosin Va and is sufficient to explain the inhibition of full-length myosin Va motor activity under physiological ionic conditions (12–14).

The GTD-deleted constructs such as McM5ΔT and M5-1105 formed a T- or Y-shaped structure in the absence of GTD, but these molecules adopt a triangular shape in the presence of GTD (Fig. 7) that is similar to the triangular-shaped conformation of full-length myosin Va in the inhibited state. The GTD-induced formation of the triangular conformation was correlated with the GTD-dependent inhibition of the actin-activated ATPase activity of the truncated myosin Va. These results support the notion that the triangular conformation represents the inhibited form of myosin Va (12). This is further supported by the results showing that neither McM5ΔTΔ3 nor M5-1047 forms the triangular conformation in the presence of exogenous GTD, and this is reflected by the lack of inhibition by GTD. The results also suggest that GTD binds to the C-terminal region of coil-1. The lengths of coil-1 and the head domain of myosin Va are about 30 nm. A triangular conformation could be formed, if GTD simultaneously binds to the C terminus of coil-1 and the head domain. If so, the proper length of the neck and coil-1 would be critical for the inhibited state of myosin Va.

This view is supported by the finding that myosin Va constructs with a shortened neck (McM5ΔTΔIQ12, McM5ΔTΔIQ34, or McM5ΔTΔIQ56) are not inhibited by GTD. If GTD binds to the C terminus of coil-1, the head domain will not reach the GTD when the neck length is shortened. Furthermore, myosin Va with a shortened coil-1 (such as McM5ΔTΔ42aa) is not inhibited by GTD. This suggests that, because the neck length is sufficient to reach the GTD at the C-terminal end of the coil-1, the neck domain and the coil-1 are rigid and the matching of the length of the two domains is critical for the interaction between the motor domain and the GTD domain, thus inactivating the motor activity. Supporting this idea, the inhibition of McM5ΔTΔIQ34 by GTD was partially restored by deleting 42 amino acid residues of coil-1 (McM5ΔTΔIQ34Δ42aa in Fig. 8). The complete restoration of regulation may require appropriate orientation of the GTD and
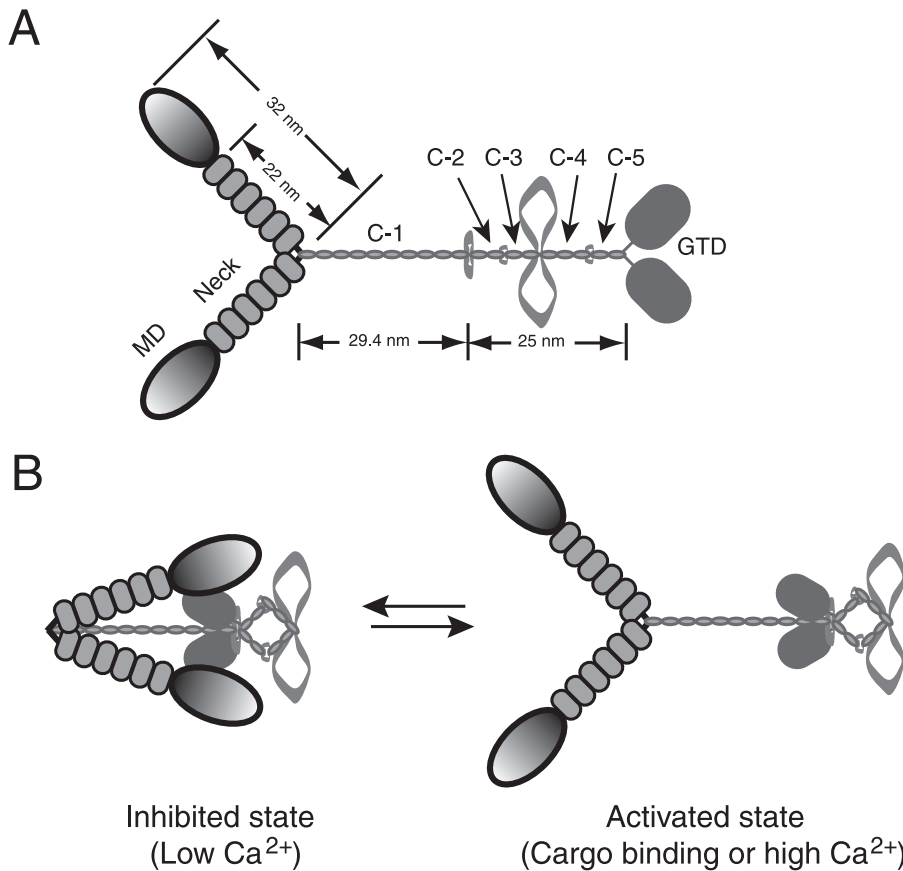
FIGURE 9. **Proposed model for the inhibited state of myosin Va.** *A*, predicted structure of myosin Va based on its sequence. At the N terminus is the motor domain (*MD*) containing the ATP and actin binding sites. The motor domain is followed by a neck that consists of six IQ motifs with the consensus sequence IQ*XXX*RG*XXX*R, which act as the binding sites for calmodulin or myosin light chains. The next ~500 amino acids are predicted to form five coiled-coils (C-1 to C-5) separated by several flexible regions. The last ~400 amino acids form a GTD. *B*, proposed structure of myosin Va in the inhibited state. At low Ca^{2+} conditions, GTD binds to the C-terminal end of the coil-1. The coil-2 to coil-5 region forms a compact structure that is visualized as a small globular domain (Fig. 5*A*). The binding of the motor domain to the GTD associated at the C-terminal end of the first coiled-coil stabilizes an isosceles triangle conformation, and prevents the conformational changes of the motor domain during the ATP turnover cycle; thus inhibiting the ATPase activity of motor domain. The activated state can be achieved by cargo binding and/or elevation of Ca^{2+}. Cargo binding to the tail domain may interfere with the interaction between GTD and head, thus disrupting the triangular shape. High Ca^{2+} stimulates the actin-activated ATPase activity and induces an extended conformation of myosin Va, presumably through the calmodulin bound to the IQ motifs (see "Discussion" for details).

of myosin Va was enhanced by its cargo-binding protein, melanophilin (17). Whereas a number of cargo molecules can bind to myosin Va, it is unlikely that these cargo molecules always disrupt the inhibited form. Ca^{2+}-dependent activation may play a role for the transport of such cargo molecules. It has been shown that micromolar concentrations of Ca^{2+} stimulates the actin-activated ATPase activity and induces an extended conformation of myosin Va (12–14). The activation by Ca^{2+} is presumably through calmodulin bound to the IQ motifs. It is possible that the neck region, especially the calmodulin bound to the 1st IQ motif, is involved in the binding of GTD to the head. High Ca^{2+} may change the conformation of calmodulin at this motif, thus disrupting its interaction with GTD. Alternatively, the triangular conformation of myosin Va may require the proper interaction between calmodulins bound to the 6th IQ motif at the joint of the each heads, which is disrupted by high Ca^{2+}. Another possibility is that high Ca^{2+} induces the dissociation of calmodulin from IQ motifs, thus compromising the structure of neck and disrupting the triangular conformation. Further studies are required to clarify this issue.

Currently, the crystal structures of three components of myosin Va, *i.e.* the motor domain (29, 30), the neck (31, 32), and GTD (33), have been solved at high resolution. The fitting of these crystal structures into the triangular conformation of myosin Va should provide detailed structural information on the inhibited state of myosin Va.

the motor domain in addition to the matched length of the coil-1 and the head domain.

Based upon the findings of the present study, we propose a model for the formation of the inhibited state of myosin Va under normal low Ca^{2+} conditions *in vivo* as follows. GTD binds to the C-terminal end of coil-1. The neck-tail junction of myosin Va is flexible, and the long neck enables the head domain to reach the GTD associated at the end of coil-1. Once the heads interact with the GTD, the triangular-inhibited conformation is stabilized. The binding of the head domain to GTD prevents its conformational change during ATP turnover or interaction with actin, thus inhibiting the actin-activated ATPase activity of the motor domain (Fig. 9). There are two scenarios to destabilize the inhibited conformation. Cargo binding to the tail domain of myosin Va in the inhibited state may interrupt the interaction between GTD and the head of myosin Va, thus shifting the conformational equilibrium toward the active state. This possibility is supported by the finding that the actin-activated ATPase activity

REFERENCES

1. Berg, J. S., Powell, B. C., and Cheney, R. E. (2001) *Mol. Biol. Cell* **12,** 780–794
2. Richards, T. A., and Cavalier-Smith, T. (2005) *Nature* **436,** 1113–1118
3. Cheney, R. E., O'Shea, M. K., Heuser, J. E., Coelho, M. V., Wolenski, J. S., Espreafico, E. M., Forscher, P., Larson, R. E., and Mooseker, M. S. (1993) *Cell* **75,** 13–23
4. Rodriguez, O. C., and Cheney, R. E. (2002) *J. Cell Sci.* **115,** 991–1004

5. Zhao, L. P., Koslovsky, J. S., Reinhard, J., Bahler, M., Witt, A. E., Provance, D. W., Jr., and Mercer, J. A. (1996) *Proc. Natl. Acad. Sci. U. S. A.* **93,** 10826–10831

6. Mehta, A. D., Rock, R. S., Rief, M., Spudich, J. A., Mooseker, M. S., and Cheney, R. E. (1999) *Nature* **400,** 590–593

7. Yildiz, A., Forkey, J. N., McKinney, S. A., Ha, T., Goldman, Y. E., and Selvin, P. R. (2003) *Science* **300,** 2061–2065

8. Forkey, J. N., Quinlan, M. E., Shaw, M. A., Corrie, J. E., and Goldman, Y. E. (2003) *Nature* **422,** 399–404

9. Burgess, S., Walker, M., Wang, F., Sellers, J. R., White, H. D., Knight, P. J., and Trinick, J. (2002) *J. Cell Biol.* **159,** 983–991

10. Walker, M. L., Burgess, S. A., Sellers, J. R., Wang, F., Hammer, J. A., 3rd, Trinick, J., and Knight, P. J. (2000) *Nature* **405,** 804–807

11. Wu, X., Bowers, B., Wei, Q., Kocher, B., and Hammer, J. A., 3rd (1997) *J. Cell Sci.* **110,** 847–859

12. Wang, F., Thirumurugan, K., Stafford, W. F., Hammer, J. A., 3rd, Knight, P. J., and Sellers, J. R. (2004) *J. Biol. Chem.* **279,** 2333–2336

13. Li, X. D., Mabuchi, K., Ikebe, R., and Ikebe, M. (2004) *Biochem. Biophys. Res. Commun.* **315,** 538–545

14. Krementsov, D. N., Krementsova, E. B., and Trybus, K. M. (2004) *J. Cell Biol.* **164,** 877–886

15. Homma, K., Saito, J., Ikebe, R., and Ikebe, M. (2000) *J. Biol. Chem.* **275,** 34766–34771

16. Wang, F., Chen, L., Arcucci, O., Harvey, E. V., Bowers, B., Xu, Y., Hammer, J. A., 3rd, and Sellers, J. R. (2000) *J. Biol. Chem.* **275,** 4329–4335

17. Li, X. D., Ikebe, R., and Ikebe, M. (2005) *J. Biol. Chem.* **280,** 17815–17822

18. Fukuda, M., Kuroda, T. S., and Mikoshiba, K. (2002) *J. Biol. Chem.* **277,** 12432–12436

19. Wu, X. S., Rao, K., Zhang, H., Wang, F., Sellers, J. R., Matesic, L. E., Copeland, N. G., Jenkins, N. A., and Hammer, J. A., 3rd. (2002) *Nat. Cell Biol.* **4,** 271–278

20. Nagashima, K., Torii, S., Yi, Z., Igarashi, M., Okamoto, K., Takeuchi, T., and Izumi, T. (2002) *FEBS Lett.* **517,** 233–238

21. Strom, M., Hume, A. N., Tarafder, A. K., Barkagianni, E., and Seabra, M. C. (2002) *J. Biol. Chem.* **277,** 25423–25430

22. Spudich, J. A., and Watt, S. (1971) *J. Biol. Chem.* **246,** 4866–4871

23. Chien, Y. H., and Dawid, I. B. (1984) *Mol. Cell. Biol.* **4,** 507–513

24. Ikura, M., Marion, D., Kay, L. E., Shih, H., Krinks, M., Klee, C. B., and Bax, A. (1990) *Biochem. Pharmacol.* **40,** 153–160

25. Stachelek, S. J., Kowalik, T. F., Farwell, A. P., and Leonard, J. L. (2000) *J. Biol. Chem.* **275,** 31701–31707

26. Mabuchi, K. (1990) *J. Struct. Biol.* **103,** 249–256

27. Burgess, S. A., Walker, M. L., Thirumurugan, K., Trinick, J., and Knight, P. J. (2004) *J. Struct. Biol.* **147,** 247–258

28. Berger, B., Wilson, D. B., Wolf, E., Tonchev, T., Milla, M., and Kim, P. S. (1995) *Proc. Natl. Acad. Sci. U. S. A.* **92,** 8259–8263

29. Coureux, P. D., Sweeney, H. L., and Houdusse, A. (2004) *EMBO J.* **23,** 4527–4537

30. Coureux, P. D., Wells, A. L., Menetrey, J., Yengo, C. M., Morris, C. A., Sweeney, H. L., and Houdusse, A. (2003) *Nature* **425,** 419–423

31. Terrak, M., Wu, G., Stafford, W. F., Lu, R. C., and Dominguez, R. (2003) *EMBO J.* **22,** 362–371

32. Terrak, M., Rebowski, G., Lu, R. C., Grabarek, Z., and Dominguez, R. (2005) *Proc. Natl. Acad. Sci. U. S. A.* **102,** 12718–12723

33. Pashkova, N., Jin, Y., Ramaswamy, S., and Weisman, L. S. (2006) *EMBO J.* **25,** 693–700